HAL open science

Chemical durability evaluation of silver phosphate based glasses designed for the conditioning of radioactive iodine

Anne-Lise Chabauty, François Mear, Lionel Montagne, Lionel Campayo

To cite this version:

Anne-Lise Chabauty, François Mear, Lionel Montagne, Lionel Campayo. Chemical durability evaluation of silver phosphate based glasses designed for the conditioning of radioactive iodine. Journal of Nuclear Materials, 2021, 550, pp.152919. 10.1016/j.jnucmat.2021.152919 . cea-03579834

HAL Id: cea-03579834

https://cea.hal.science/cea-03579834v1

Submitted on 22 Mar 2023

HAL is a multi-disciplinary open access archive for the deposit and dissemination of scientific research documents, whether they are published or not. The documents may come from teaching and research institutions in France or abroad, or from public or private research centers.

L'archive ouverte pluridisciplinaire **HAL**, est destinée au dépôt et à la diffusion de documents scientifiques de niveau recherche, publiés ou non, émanant des établissements d'enseignement et de recherche français ou étrangers, des laboratoires publics ou privés.

Distributed under a Creative Commons Attribution - NonCommercial 4.0 International License

Version of Record: https://www.sciencedirect.com/science/article/pii/S0022311521001434
Manuscript_b353ff070a6d38c1c8971a67dc6cd060

Chemical durability evaluation of silver phosphate–based glasses designed for the conditioning of radioactive iodine

A.-L. Chabauty[1, 2], F. O. Méar[1], L. Montagne[1], L. Campayo[2*]

(1) Univ. Lille, CNRS, Centrale Lille, Univ. Artois, UMR 8181 - UCCS - Unité de Catalyse et Chimie du Solide, F-59000 Lille, France.

(2) CEA, DES, ISEC, DE2D, University of Montpellier, Marcoule, F-30207 Bagnols-sur-Cèze, France.

* Corresponding author: lionel.campayo@cea.fr

© 2021 published by Elsevier. This manuscript is made available under the CC BY NC user license
https://creativecommons.org/licenses/by-nc/4.0/

Highlights

- Iodine-containing phosphate-based glasses are compared in terms of durability.
- Phosho-molybdate glasses are more durable than phosphate glasses in pure water.
- Nb_2O_5 improves the chemical durability of phospho-molybdate glasses.
- Acidic conditions seem detrimental to the durability of these conditioning matrices.

Abstract

Silver phosphate glasses have been investigated for the conditioning of radioactive iodine 129. Their disposal in a deep geological repository requires high chemical durability, and to improve this property, two crosslinking agents were examined here: Nb_2O_5 and Bi_2O_3. In addition, for some of these glasses, 50 % of phosphorus was replaced by molybdenum to assess the role of glass former entities. The effect of these modifications on the glass chemical durability was studied in pure water, at 50 °C. Given the very long half-life of iodine 129 (15.7 x 10^6 years), only long-term alteration tests were carried out, in order to check if a passivating alteration layer could be formed in these conditions. Alteration rates were then calculated following various methods and compared. Results showed that the use of elemental releases in solution alone leads to an underestimation of the alteration rate, as there is no tracer element in the glass composition. For phospho-molybdate glasses, the addition of Nb_2O_5 had a significant effect on their chemical durability, i.e. their ability to form a passivating layer that retains most of the elements that are part of the pristine glass. For phosphorus, the more mobile element, release rates decreased by two orders of magnitude compared to phosphate-only glasses, and this trend depends on the Nb_2O_5 concentration.

Keywords

Silver phosphate glasses; Radioactive iodine; Nuclear waste conditioning; Chemical durability

1. Introduction

Radioactive waste produced by nuclear power plant electricity generation must be managed in order to minimize its impact on the environment and on human health. High level nuclear waste is usually vitrified in borosilicate glasses in anticipation of their storage in a deep geological repository [1]. However some waste, such as iodine 129, requires special management due to its low incorporation rate in this matrix [2]. Currently, one of the common management strategies for this isotope relies on its isotopic dilution in sea water. An alternative solution based on a conditioning matrix is considered here, in order to decrease its environmental impact.

As a part of the reprocessing of spent nuclear fuels, iodine can be trapped on silver nitrate-impregnated filters [3]. It can then be easily recovered as silver iodide [4]. However, considering the high volatility of iodine (silver iodide is volatile above 650 °C [5]), the usual vitrification process cannot be applied, as nuclear borosilicate glasses require melting at least at 1100 °C [6].

Due to their lower melting temperature, as well as their ability to incorporate high amounts of iodine (up to 65 mol% AgI) [7], phosphate glasses, and especially silver phosphate glasses, have been suggested for the specific conditioning of radioactive iodine [8][9]. However, phosphate-only glasses are also known to be less resistant to alteration in an aqueous medium than borosilicate glasses, and therefore they could not be considered as suitable for long-term storage in a geological repository. Consequently, several studies have been carried out to understand the alteration mechanism of silver phosphate glasses and to improve their chemical durability [10][11][12]. One of the methods implemented to reach this goal

includes the addition of crosslinking reagents to the glass composition, in order to increase glass network connectivity. However, previous works have shown a need to optimize these glass compositions, as crystals containing the crosslinking reagents are likely to be formed in the presence of iodine [13][14]. In addition, virtually no chemical durability assessment had been performed on these compositions.

We therefore decided to study the impact of two crosslinking reagents (Bi_2O_3 and Nb_2O_5) on the chemical durability of set of silver phosphate glasses for which no crystallization was observed. Considering the very long half-life of radioactive iodine ^{129}I (15.7 x 10^6 years), and the fact that it is highly mobile in the geological environments generally considered for storage purposes [15], the long-term chemical durability of the chosen matrix is of critical importance. Although a complete understanding of glass corrosion in radioactive waste geological repositories is not available yet, it has often been described by a sequence of different alteration steps. A hydration step in the presence of water vapor is thought to occur first. However, the decay of iodine 129 is not responsible for a strong heat output, and this step might not concern such materials. Then for saturated conditions, models take into account the dissolution of glass components followed by the formation of an alteration layer, and transport through this layer [16]. Such models were first developed for borosilicate glass, but are thought to possibly extend to phosphate glasses [17]. For particular alteration conditions (high pH values), an alteration resumption could also play a role in elemental releases [18], but to our knowledge, this topic was not investigated for phosphate glasses. For the borosilicate glasses designed for the conditioning of HL waste, transport through an alteration layer is thought to account for the long-term durability of such a matrix [19]. We assume that this statement can also be applied to the glasses studied here. More specifically, the chosen matrix must display a drop in the alteration rate to reach a low residual

alteration state which will drive its long-term behavior. This drop is observed when an alteration layer exhibiting protective diffusive properties develops at the pristine glass / solution interface. In order to reveal such a drop, alteration tests must be carried out with a high S/V (surface of glass to volume of solution) ratio.

From previous results on microstructural studies [13][14], two first sets of compositions were chosen: namely, $AgPO_3$ (Ag/P = 1) and $Ag_5P_3O_{10}$ (Ag/P = 1.6)–based glasses. A third set of compositions was also added, in which 50% of the phosphorus was replaced by molybdenum, noted as $Ag_5P_{1.5}Mo_{1.5}$ (Ag/(P+Mo) = 1.6) (abbreviation for $Ag_5P_{1.5}Mo_{1.5}O_{10.75}$ – based glass). In order to be able to compare the results, the same minimum amount of crosslinking reagent was added for each composition: 2 mol%, before iodine addition (equivalent to 1.6 mol% after iodine addition). Molybdenum was added to the glass composition as a second glass former in order to try to counterbalance the very acidic conditions generated during alteration of phosphate-only glasses, and assess the influence of pH.

2. Materials and Method

2.1. Glass synthesis

The silver phosphate glasses were prepared using analytical grade AgI (Alfa Aesar, 99.9%), $AgNO_3$ (Alfa Aesar, 99.9%), $(NH_4)_2HPO_4$ (Prolabo, 97.5%), MoO_3 (Alfa Aesar, 99.95%), Nb_2O_5 (Alfa Aesar, 99.5%), and Bi_2O_3 (Aldrich, 99.9%). Nb_2O_5 and Bi_2O_3 have been used in the past as crosslinking reagents to strengthen the glass network by increasing connectivity between glass former entities (either phosphate or molybdate in the current case) [13]. Three series/systems were studied here, noted as AgI-$AgPO_3$, AgI-$Ag_5P_3O_{10}$, and AgI-$Ag_5P_{1.5}Mo_{1.5}$

(Table 1). For each system, the influence of the crosslinking reagents was investigated. In order to obtain homogeneous glasses, a two-step synthesis was performed. During the first step, all the reagents except for AgI were heated in a Pt/Au crucible up to 600°C at a heating rate of 1°C/min. After being held at 600°C for 3h to remove the nitrate, hydroxyl, and ammonium groups, the temperature was raised to 900°C at a heating rate of 5°C/min, and maintained for 1h. To ensure a fast cooling and to limit any crystallization process, the melt was then cast between two brass plates in order to maximize heat transfer. The iodine glass was prepared in a second step, during which the previously AgI -free glass was mechanically ground, mixed with AgI (weighted to reach 12 wt.% of iodine), and heated at 650°C for 1h. Once again, the melt was cast between two brass plates. After cooling, the glass compositions (Table 1) were checked on polished samples by EDS (see § II.3. Characterization techniques for details). Results showed that there was no iodine volatilization during the process.

Sample name	**Theoretical glass composition (mol%)**					**Theoretical batch *(measured)* composition (wt.%)**					
	AgI	**Ag_2O**	**P_2O_5**	**Nb_2O_5**	**Bi_2O_3**	**I (± 1 wt.%)**	**Ag (± 1 wt.%)**	**P (± 1 wt.%)**	**Nb (± 0.1 wt.%)**	**Bi (± 0.1 wt.%)**	**O (± 1 wt.%)**
AgI-$AgPO_3$	18.5	40.7	40.7	-	-	12.0 *(12.4)*	55.1 *(55.8)*	12.9 *(12.1)*	-	-	20.0 *(19.7)*
AgI-$AgPO_3$-$2Nb_2O_5$	18.6	39.9	39.9	1.6	-	12.0 *(12.8)*	53.8 *(52.6)*	12.5 *(12.8)*	1.5 *(1.0)*	-	20.2 *(20.8)*
AgI-$AgPO_3$-$2Bi_2O_3$	19.0	39.7	39.7	-	1.6	12.0 *(12.8)*	52.9 *(51.7)*	12.3 *(12.4)*	-	3.4 *(2.9)*	19.4 *(20.2)*
AgI-$Ag_5P_3O_{10}$	19.4	50.4	30.2	-	-	12.0 *(12.8)*	63.2 *(61.6)*	9.1 *(9.2)*	-	-	15.7 *(16.4)*
AgI-$Ag_5P_3O_{10}$-$2Nb_2O_5$	19.5	49.3	29.6	1.6	-	12.0 *(12.7)*	61.8 *(60.6)*	8.9 *(9.1)*	1.4 *(1.0)*	-	15.9 *(16.6)*
	AgI	**Ag_2O**	**P_2O_5**	**MoO_3**	**Nb_2O_5**	**I (± 1 wt.%)**	**Ag (± 1 wt.%)**	**P (± 1 wt.%)**	**Mo (± 1 wt.%)**	**Nb (± 0.1 wt.%)**	**O (± 1 wt.%)**
AgI-$Ag_5P_{1,5}Mo_{1,5}$	18.7	42.8	12.8	25.7	-	12.0 *(12.8)*	56.7 *(55.3)*	4.0 *(4.0)*	12.4 *(12.3)*	-	14.8 *(15.5)*
AgI-$Ag_5P_{1,5}Mo_{1,5}$-$2Nb_2O_5$	18.9	41.8	12.6	25.1	1.6	12.0 *(13.0)*	55.4 *(53.9)*	3.9 *(4.0)*	12.1 *(12.3)*	1.5 *(1.0)*	15.1 *(15.8)*
AgI-$Ag_5P_{1,5}Mo_{1,5}$-$5Nb_2O_5$	19.1	40.5	12.1	24.3	4.0	12.0 *(13.0)*	53.5 *(52.1)*	3.7 *(3.8)*	11.6 *(11.9)*	3.7 *(3.3)*	15.4 *(16.1)*

Table 1. Composition of the glasses studied

It is worth noting that not all the crosslinking reagents (Nb_2O_5 or Bi_2O_3) are compatible with the three sets of compositions, due to solubility issues. This explains why Bi_2O_3 could not be used to increase glass network connectivity for the $Ag_5P_3O_{10}$ –based or the $Ag_5P_{1.5}Mo_{1.5}O_{10.75}$ –based glasses [14]. Such mismatching will be recalled when necessary in the results section.

2.2. Method for the chemical durability study

2.2.1. Experimental

In order to study the chemical durability of the glasses, long-term stability tests were conducted. To favor a retroactivity of the elements released by the glass on the kinetics, it was decided to conduct these tests in static mode (there was no renewal of the alteration solution during the tests) and the glass surface to solution volume (S/V) was high. These conditions were selected to promote the formation of a passivating layer, if such a layer could develop. All experiments were carried out in temperature-controlled ovens (precision of ± 1°C), using polytetrafluoroethylene (PTFE) reactors (Figure 1).

To promote the appearance of a residual alteration state due to the formation of a passivating layer, the S/V ratio was fixed at 80 cm^{-1}, which can favor saturation of the solution. To obtain this ratio, a sufficient amount of glass was ground, then sieved, to collect the 20-40 µm fraction. This fraction was ultrasonically cleaned in ethanol and acetone to remove any small particles that could have adhered to the grain surface during the grinding process. The glass surface area was determined by the BET method using N_2 as a probe (*Micrometrics Gemini 2360*). The exact amount of glass needed was then weighed and placed in a reactor containing 100 mL of ultra-pure water heated to 50°C. One or two glass monoliths were also added to the reactor so that the alteration layer formed could be better characterized. The surface area of the monoliths was approximately 100 mm^2, which is far

below the surface area of the glass powder (about 0.8 m²), meaning that the release of elements by the glass monolith could be ignored during the alteration rate calculation. Then the reactor was put in a ventilated oven heated to 50°C for at least 56 days. To promote a saturation phenomenon and the formation of an alteration layer, there was no stirring during the test. Solution aliquots (~ 2 mL with no renewal of solution) were taken from the reactor at regular intervals, and the pH was monitored. At the end of the test, the solution was filtered to recover the glass powder, which was dried for 24h at 100°C and then observed by SEM and analyzed by XRD. The glass monoliths were also studied by SEM, in order to determine the thickness of the alteration layer. Finally, the solution samples were analyzed by ICP-MS to determine the concentration of the glass elements released in solution, with a 3% uncertainty. Two samplings were carried out for each duration: a first that was acidified with HNO_3 (0.1 N) for cation analysis, and a second with no acid addition for iodine analysis.

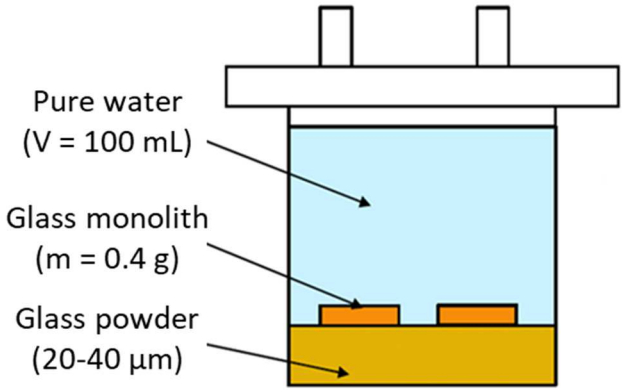

Figure 1. Reactor used for the long-term stability study

2.2.2. Alteration rate calculation

Two methods were used to calculate the alteration rate.

Using elemental releases in solution

The alteration rate was first calculated using the release of the glass elements in solution. This method requires the availability of tracer elements which do not precipitate in secondary phases and/or are not part of the alteration layer, whether or not this layer is passivating. When several elements can be used as tracers, glass former elements have to be preferred, as they are more representative of the glass network alteration.

Using the concentration of a tracer element in the alteration solution, normalized mass loss (NML) can be calculated according to the following equation (1) derived from the shrinking core model used by Jegou et al. in [16]:

$$NML_i(g.m^{-2}) = \frac{3*(1-(1-alt_i)^{1/3})}{S_{BET}} \quad \textit{(Equation 1)}$$

Where:

-NML_i is the normalized mass loss calculated for the element named “i”, in $g.m^{-2}$

-S_{BET} is the surface area measured by the BET method, in $m^2.g^{-1}$

-alt_i is the altered fraction of the glass given by equation (2):

$$alt_i = \frac{C_i^t * V^t + \ {}_{a=1}^{t-1} c_i^a * v^a}{m_{glass} * f_i} \qquad \textit{(Equation 2)}$$

Where:

-t is the duration, in days, between the beginning of the test and the sampling

-C_i^t and V^t are the concentration of element i and the volume of sampled solution at time t, respectively

-m_{glass} is the initial weight of glass placed in the reactor

-f_i is the weight fraction (percentage) of element "i" in the glass at the beginning of the test.

From the NML, the alteration rate R (given in $g.m^{-2}.d^{-1}$) can be calculated using Equation 3:

$$R = \frac{NML_{i,t} - NML_{i,tstart}}{t - t_{start}} \qquad \textit{(Equation 3)}$$

Alteration rates calculated using this method are usually given with a 20% uncertainty. Only the last 4-5 points of each curve were used for this calculation, to ensure the presence of an alteration layer.

Using the thickness of the alteration layer

If no tracer element is available, the alteration rate can be calculated on the basis of the thickness of the alteration layer. In this case, the assumption is made that the whole alteration phenomenon is isovolumic, as it is often the case in this field [17]. The alteration layer, observed by SEM (see § II.3. Characterization techniques for details), can be measured using an image processing software [18]. Considering the irregularity of the layers, 20 measurements were taken for each sample and an average thickness was deduced. The alteration rate was then calculated using Equation 4:

$$\mathrm{R} = \frac{ETh \times \rho}{t} \qquad \textit{(Equation 4)}$$

Where:
-R is the alteration rate, given in $g.m^{-2}.d^{-1}$
-ETh is the measured equivalent thickness of the alteration layer, in µm
- ρ is the density of the glass, in $g.cm^{-3}$
-t is the total duration of the test

An average density was used, based on the values reported by *Lemesle et al.* [11]. For similar amounts of iodine to those involved here, they reported average density values of 5 $g.cm^{-3}$ for the AgI-$AgPO_3$ system, and of 5.5 $g.cm^{-3}$ for the AgI-$Ag_5P_3O_{10}$ system. They also showed that the addition of a crosslinking reagent had only a low impact on the glass density.

2.3. Characterization techniques

The compositions of glassy fractions and crystalline phases were determined by quantitative analysis using EDS (Bruker AXS X-Flash Detector 4010 system) on polished samples mounted in epoxy resin and polished with silicon carbide discs up to a 4000 grade and a mirror–like finish, obtained with a 1 µm-diamond paste. These quantifications use certified standards using the classic PhiRhoZ method on a *Zeiss Supra™ 55* SEM, operating at 15 kV with a probe current of 1 nA. The crystallinity of ground samples was checked by X-ray Diffraction at room temperature with a Panalytical MPD Pro fitted with a copper anode using Cu Kα radiation ($K_{\alpha 1}$=1.54056 Å) generated at 40 mA and 40 kV. The 2θ range between 10 and 70° was used, and was scanned with 0.017° steps. Diffractograms were analyzed using the EVA version 10.0 rev. 1 program (DIFRACTplus, Bruker).

A Time-of-Flight Secondary Ion Mass Spectrometer (ToF-SIMS) (TOF5, IONTOF GmbH, Münster, Germany) was used to obtain elemental depth profiles. Two sputtering beams abrading a surface area of 200 × 200 μm^2 were used: a 2000 eV - 50 nA Cs^+ beam when analyzing anions, and a 2000 eV - 560 nA O_2^+ beam when analyzing cations. The anions and cations were analyzed using a Bi^+ 25 keV ion beam at 1.5 pA over an area measuring 50 × 50 μm^2. The surface charges created during the analyses were neutralized using a pulsed low-energy (< 20 eV) electron flux. The depth calibration was carried out using the abrasion rate and a mechanical profilometer to measure the crater depth at the end of the analysis. It should be noted that the same abrasion rate was used for analyzing the gel layer and the pristine glass.

3. Results

3.1. AgI-$AgPO_3$ system

For the $AgPO_3$ set, both Nb_2O_5 and Bi_2O_3 were successfully used as crosslinking reagents.

3.1.1. Altered solid analysis

Both powder and monoliths were analyzed, except for the AgI-$AgPO_3$-$2Nb_2O_5$ glass. For the latter glass, the monolith had in fact “disappeared” during the test. SEM images (BSE mode) of the AgI-$AgPO_3$ glass system (with or without crosslinking reagent) after alteration are shown in Figure 2. For the AgI-$AgPO_3$-$2Nb_2O_5$ glass, powder analysis showed that alteration had spread over the entire width of the grains, only leaving a shell as a reminder of the primary grain. While the monolith for the AgI-$AgPO_3$-$2Bi_2O_3$ glass was recovered, the SEM image shows that the grains were also fully altered, only leaving empty shells. The observation of the altered layer shows that it is quite porous and non-adhesive. Concerning the reference glass, AgI-$AgPO_3$ glass, which contained no crosslinking reagent, it can be noticed that the grains are not fully altered. The alteration layer is however also porous and non-adhesive. As such, these alteration layers do not seem to be able to play any protective role.

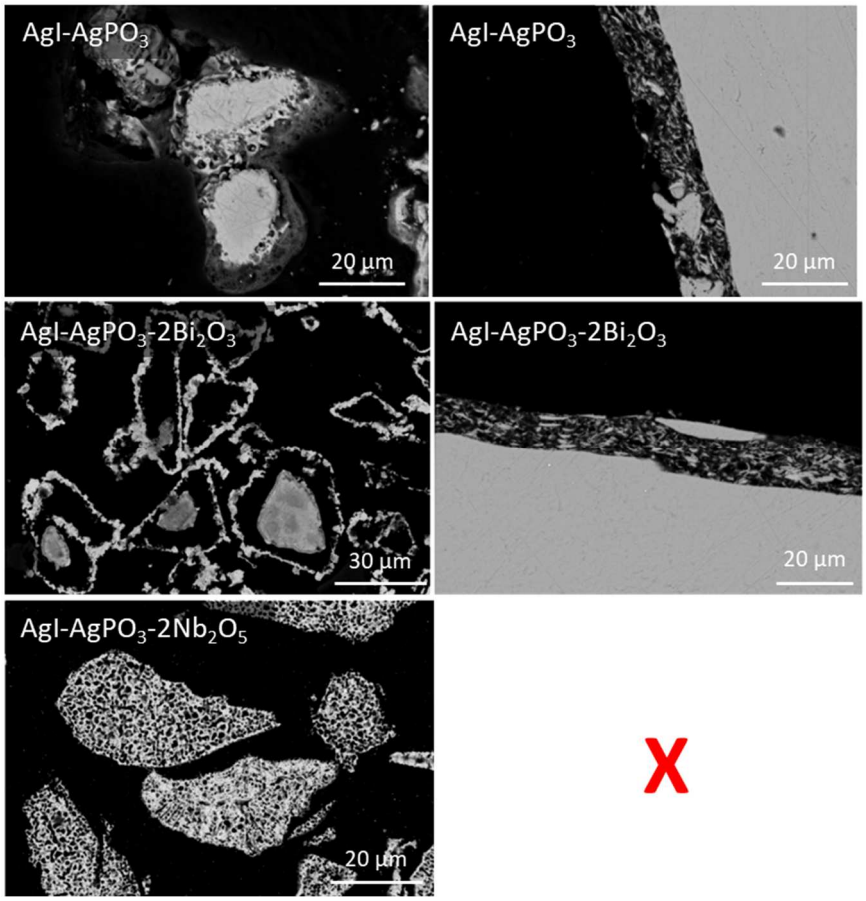

Figure 2. Backscattered electron SEM images of the AgI-$AgPO_3$ glass system (powder (left side) and monoliths (right side), when recovered) after alteration.

XRD analyses (see supplementary materials, Figure S1) of the altered glass powder revealed the presence of the $Ag_5(P_2O_7)I$ (ICDD-card: 04-013-3975) crystallized phase for the AgI-$AgPO_3$ and AgI-$AgPO_3$-$2Bi_2O_3$ glasses, as well as $BiPO_4$ (ICDD-card: 00-015-0766) for the bismuth containing glass. As all the elements originally contained in these glasses had precipitated in secondary phases, none of them could be used as tracer elements. The alteration rate calculated based on the NML (normalized mass losses) would then underestimate the actual value. Concerning the AgI-$AgPO_3$-$2Nb_2O_5$ glass, no crystalline phase was detected by XRD (see supplementary materials, Figure S1). However, an X-ray elemental mapping of this glass after alteration (Figure 3) showed that the residues left after full alteration of the grains contained all the elements of the initial glass. Therefore, none of them could be used as a tracer element either.

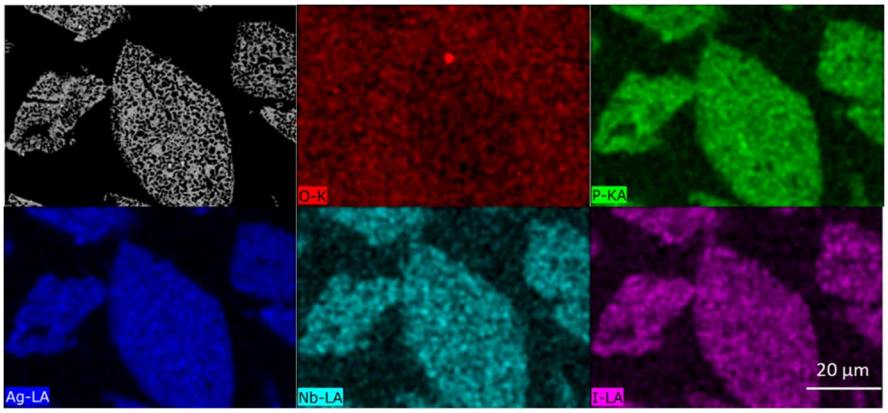

Figure 3. **X-Ray elemental mapping of the AgI-$AgPO_3$-$2Nb_2O_5$ glass powder after alteration.**

3.1.2. Solution analysis

The evolution of pH during the alteration test and of the normalized mass losses (NML) calculated for glasses of the AgI-$AgPO_3$ system are shown in Figure 4. It can be noted that the NML based on niobium release is not given here, as its concentration was below the detection limit in each case (i.e. <0.1 $mg.L^{-1}$ for our conditions). Concerning bismuth, after 7 days, it too was no longer detected, which is consistent with the precipitation of a $BiPO_4$ phase. The reason why iodine was not detected in solution can be explained by the precipitation of $Ag_5(P_2O_7)I$, but also by acidic pH values below 3.0. It is known that for very low pH values, typically below 3.0, iodine can be found as I_2, which can de-gas from the solution due to a very low solubility [19]. When examining the evolution of the NML, it can be noticed that a slight drop in the alteration rate can be observed after ten days for any of the three glasses, but this drop could be due to the precipitation of several by-products as mentioned previously.

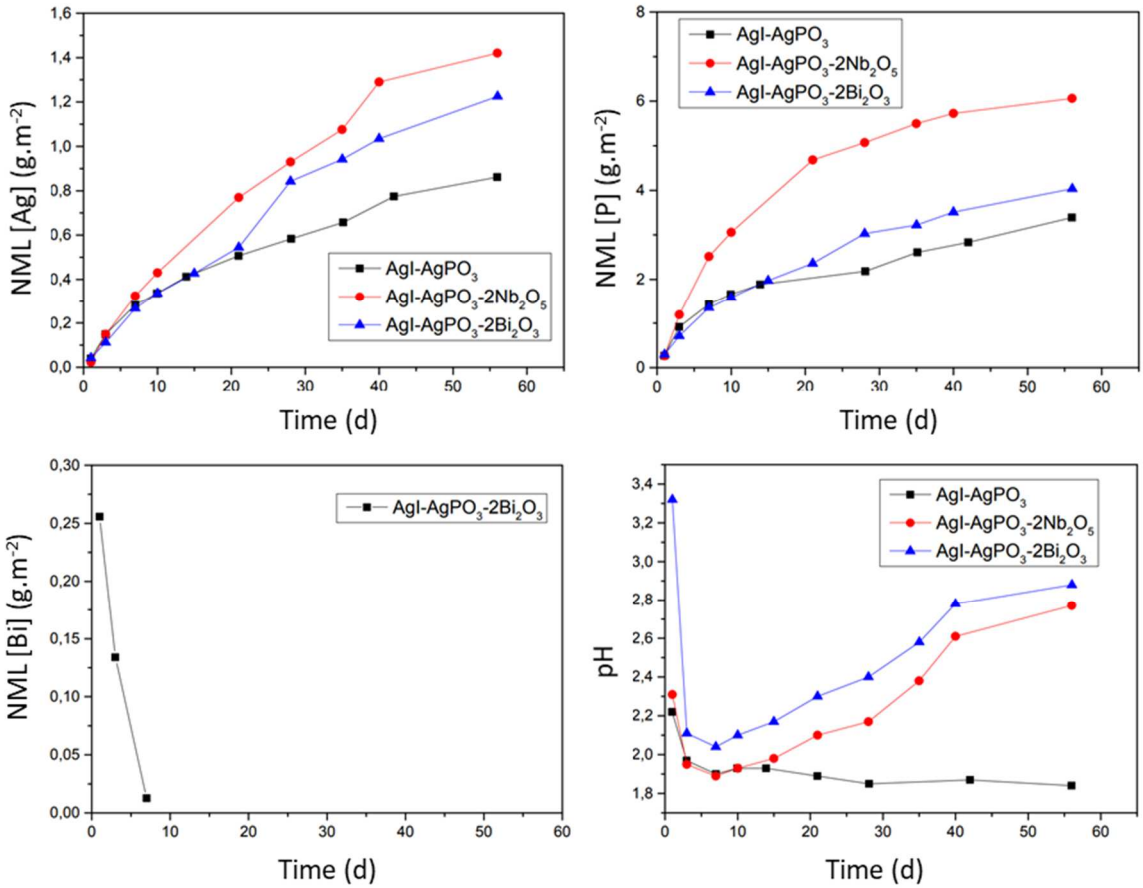

Figure 4. Normalized mass loss calculated based on the release of silver, phosphorus, and bismuth (uncertainty: 15%), and pH evolution (uncertainty: +/- 0.1) as a function of the alteration duration for glasses of the AgI-$AgPO_3$ system.

3.2. AgI-$Ag_5P_3O_{10}$ system

As the maximum amount of Bi_2O_3 that could be incorporated in the $Ag_5P_3O_{10}$ set has been shown to be lower than 1.6 mol% after iodine addition [14], only the effect of Nb_2O_5 on the chemical durability was studied for this set of compositions.

3.2.1. Altered solid analysis

SEM images (BSE mode) of glasses belonging to the AgI-$Ag_5P_3O_{10}$ system after alteration are shown in Figure 5. For these two glasses, the monoliths were recovered and could be observed as planned. The images show that grains have not been totally altered, as a core of pristine glass can still be observed. The altered layers, as seen on the monoliths, are very

porous, with no adhesion to the glass. Like the AgI-$AgPO_3$ system glass results, they do not seem to play any protective role. XRD analysis of the altered glass powder indicated that an $Ag_5(P_2O_7)I$ phase (ICDD-card: 04-013-3975) was formed during the alteration of the AgI-$Ag_5P_3O_{10}$ glass (see supplementary materials, Figure S2), meaning that there was no tracer element in this glass. Concerning the niobium -bearing glass, an $AgNbO_3$ phase was identified (ICDD-card: 04-001-8644) (see supplementary materials, Figure S2). As a consequence, silver and niobium were not used as tracer elements.

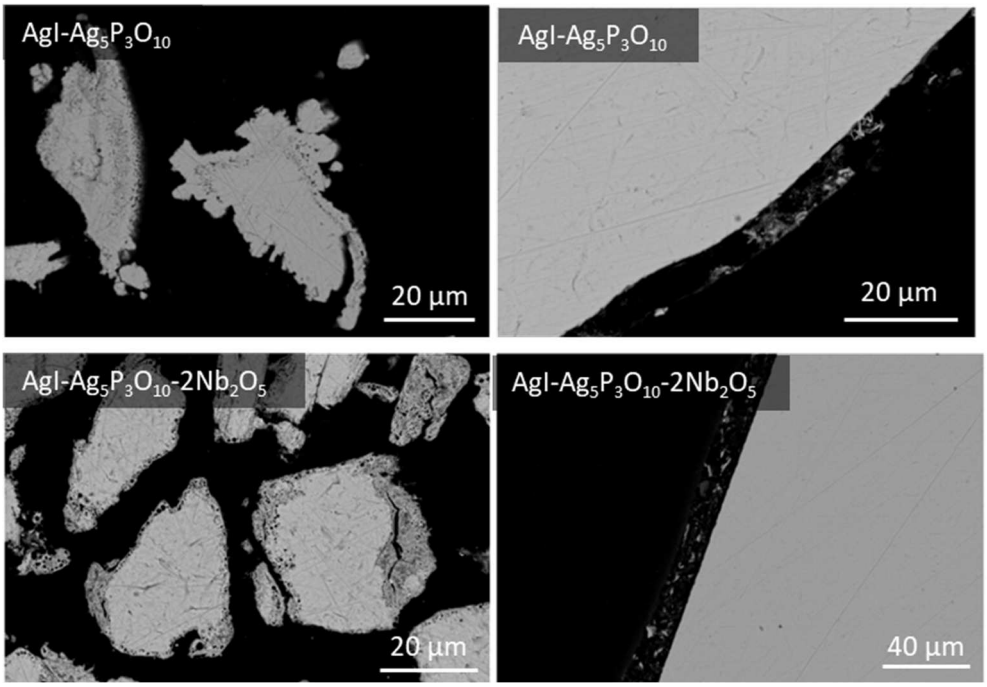

Figure 5. Backscattered electron SEM images of glasses of the AgI-$Ag_5P_3O_{10}$ system glasses (powder and monoliths) after alteration.

3.2.2. Solution analysis

The evolution of the pH during alteration and of normalized mass losses (NML) calculated for glasses of the AgI-$Ag_5P_3O_{10}$ system are shown in Figure 6. Niobium and iodine were below the detection limits (i.e. <0.1 $mg.L^{-1}$ for our conditions), which can be explained by $AgNbO_3$ precipitation, and by the very low pH values of the solutions, respectively. As was the case for the AgI-$AgPO_3$ system glasses, there was no significant drop in the alteration rate, and

thus no residual alteration regime, for either of these glasses. Once again, this is consistent with the porous feature of the alteration layers. Assuming that phosphorous could be a tracer element for the AgI-$Ag_5P_3O_{10}$-$2Nb_2O_5$ glass and that its release is underestimated for the AgI-$Ag_5P_3O_{10}$ glass, when looking at the NML it can be noted that the niobium-containing glass seems to be altered more slowly than the niobium-free sample.

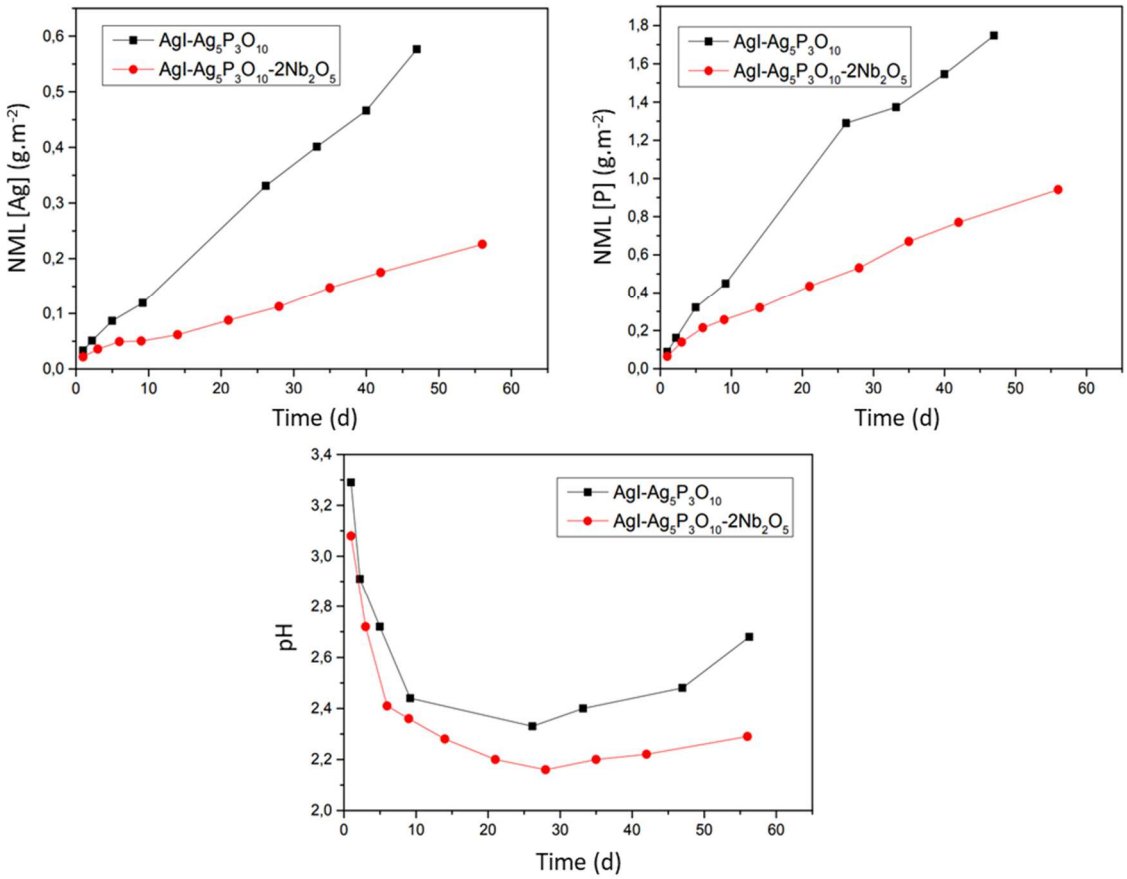

Figure 6. Normalized mass loss calculated based on the release of silver and phosphorus (uncertainty: 15%), and pH evolution (uncertainty: +/- 0.1) as a function of the alteration duration for glasses of the AgI-$Ag_5P_3O_{10}$ system.

3.3. AgI-$Ag_5P_{1.5}Mo_{1.5}$ system

Exploratory tests having shown a low incorporation limit of Bi_2O_3, only the effect of Nb_2O_5 on the chemical durability was studied for this set of compositions. It must be noted that the

maximal amount of Nb_2O_5 that could be incorporated in this particular set of compositions was higher than for the two other sets, at up to 5 mol% of Nb_2O_5 (glass without iodine).

3.3.1. Altered solid analysis

SEM images (BSE mode) of the AgI-$Ag_5P_{1.5}Mo_{1.5}$ system glasses after alteration are shown in Figure 7. Like the AgI-$Ag_5P_3O_{10}$ system glasses, all monoliths were recovered. Images show that the alteration is limited, in particular for the niobium-containing glasses. The AgI-$Ag_5P_{1.5}Mo_{1.5}$ glass displays an alteration layer that does not seem to adhere to the grains. Concerning the niobium-containing glasses, no alteration layer seems to be visible. Some small crystals could still be noticed on the edge of the AgI-$Ag_5P_{1.5}Mo_{1.5}$-5Nb_2O_5 monolith, but due to their very small size, as well as their instability under the electronic beam, these crystals could not be analyzed. XRD analyses revealed the presence of $AgNbO_3$ (ICDD-card: 04-001-8644) for both the niobium-containing glasses after alteration (see supplementary materials, Figure S3). They also revealed the presence of both Ag_2MoO_4 (ICDD-card: 00-008-0473) and $Ag_4I(PO_4)$ (ICDD-card: 00-059-0102) phases in the AgI-$Ag_5P_{1.5}Mo_{1.5}$ glass after alteration (see supplementary materials, Figure S3), meaning that there was no tracer element for this glass. Concerning the niobium-containing glasses, only Ag and Nb were discarded as tracer elements based on these results. Finally, a very light demarcation line (materialized as a red dotted line in Figure 7) can be noticed at about 2 µm below the external surface for the AgI-$Ag_5P_{1.5}Mo_{1.5}$-5Nb_2O_5 monolith. EDS quantitative analyses showed no difference in composition between the two sides of the line. This demarcation is however barely visible, and only on certain parts of the sample.

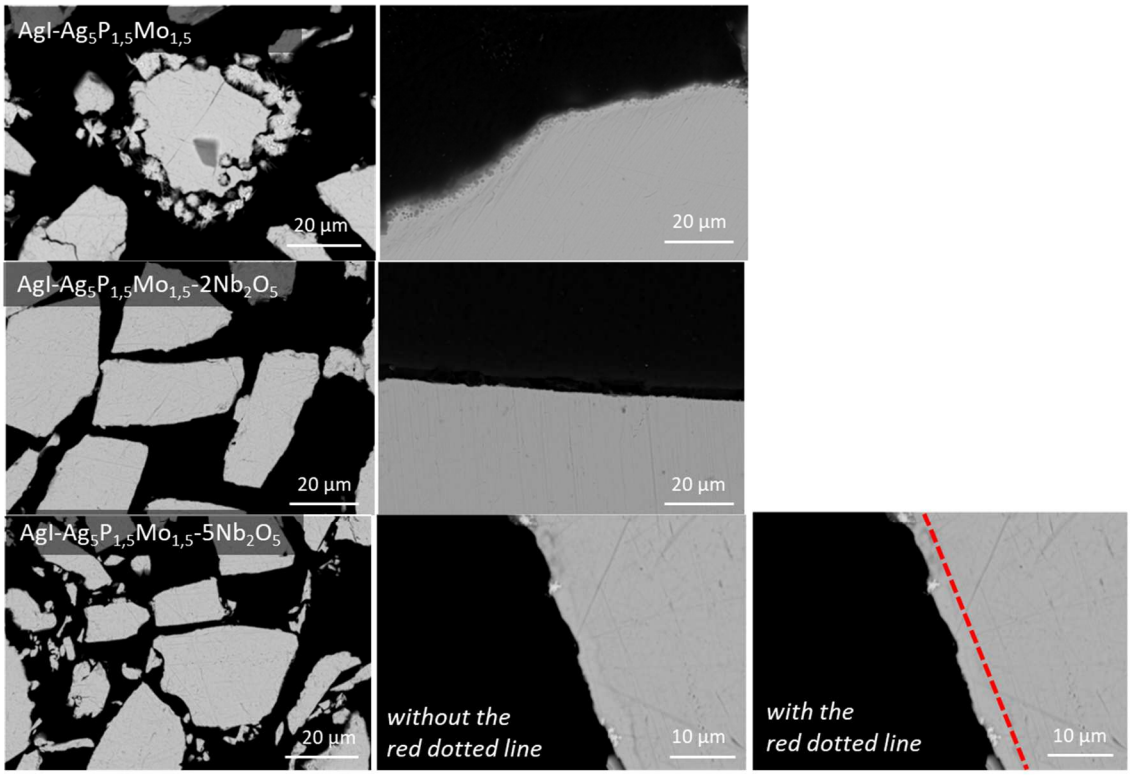

Figure 7. Backscattered electron SEM images of the AgI-$Ag_5P_{1.5}Mo_{1.5}$ system glasses (powder and monoliths) after alteration (the red dotted line indicates a barely visible demarcation (see text)).

3.3.2. Solution analysis

The evolution of the pH during alteration and of the normalized mass losses (NML) calculated for the AgI-$Ag_5P_{1.5}Mo_{1.5}$ system glasses are shown in Figure 8. As before, niobium and iodine were below their detection limits (i.e. <0.1 mg.L^{-1} for our conditions), which for niobium can once again be explained by $AgNbO_3$ precipitation. For iodine, the absence of a measurable concentration could be due to the precipitation of $Ag_4I(PO_4)$ for the AgI-$Ag_5P_{1.5}Mo_{1.5}$ glass, but for the niobium-containing glasses, no iodine was found in crystallized phases, and the pH values were too high to account for I_2 formation. This would mean that the quantity of iodine released in solution, probably in its iodide form, was below the detection limit (i.e. <0.1 mg.L^{-1} for our conditions).

Looking more closely at the results, it can be seen that the pH values are higher than for phosphate-only glasses (the AgI-$AgPO_3$ or the AgI-$Ag_5P_3O_{10}$ systems), in particular for the niobium-containing glasses. Concerning the NML, while AgI-$Ag_5P_{1.5}Mo_{1.5}$ seems to display a significant drop in the alteration rate, such a behavior can be explained by the precipitation of Ag_2MoO_4 and $Ag_4I(PO_4)$ during the test. As stated before, no tracer element exists for this peculiar composition, and therefore the alteration rate cannot be deduced from NML. Concerning niobium-containing glasses, there is no visible significant drop in the alteration rate. However, given the low alteration rate of these glasses compared to that observed for the first samplings of AgI-$Ag_5P_{1.5}Mo_{1.5}$, it might be possible that the residual alteration regime had been reached before the first sampling (1 day). This hypothesis seems to be confirmed by the very low values calculated for the NML, as well as by observations of the glasses after alteration.

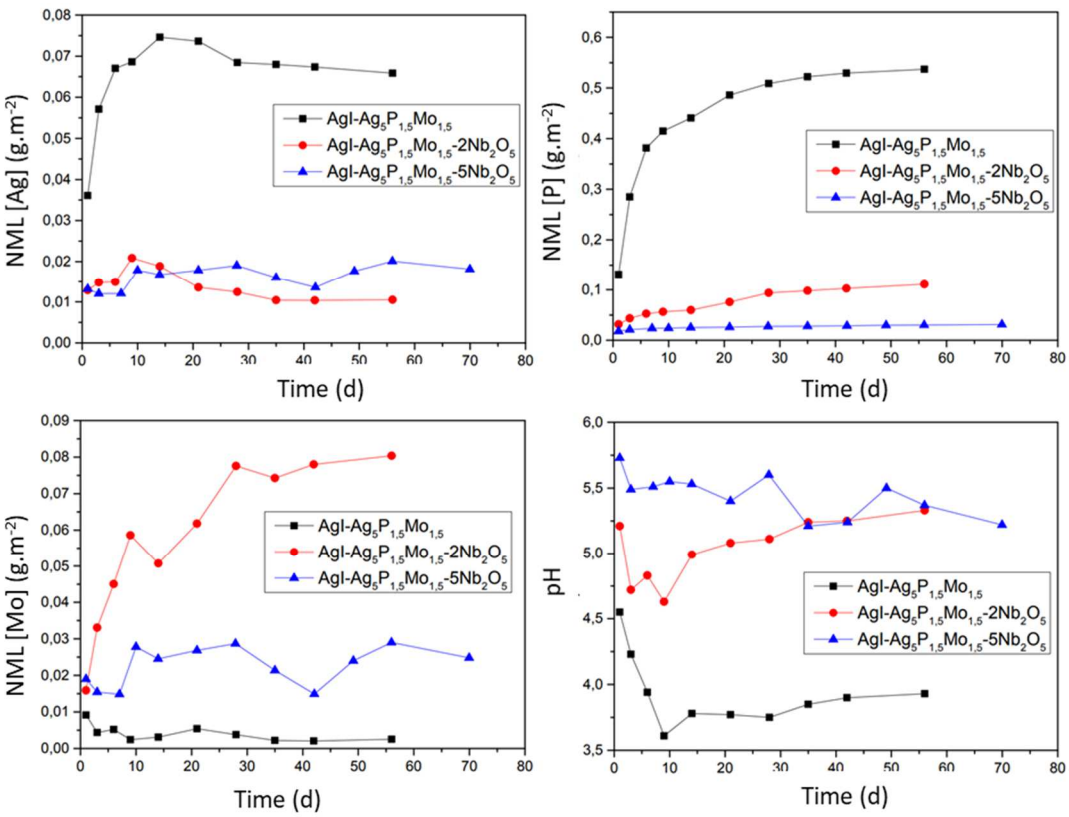

Figure 8. Normalized mass loss calculated based on the release of silver and phosphorus (uncertainty: 15%), and pH evolution (uncertainty: +/- 0.1) as a function of the alteration duration for glasses of the AgI-$Ag_5P_{1.5}Mo_{1.5}$ system.

4. Discussion

4.1. Comparison of the alteration rate calculation methods

The alteration rates calculated according to the methods detailed in the experimental section (see § 2.2.2.) are given in Table 2. While it has been noted that there was no tracer element for a majority of glasses, an alteration rate can still be mathematically calculated in each case using NML. The alteration rate is calculated here using phosphorus NML, as it gives the best estimate (among other possible elements) of the lower boundary rate: it is noted R. On the other hand, the alteration rate calculated from the thickness of the alteration layer is noted R_{layer}. As there was no monolith left to determine the alteration layer thickness of the AgI-$AgPO_3$-$2Nb_2O_5$ glass, no result is reported for this particular composition. However, given that that the glass grains were fully altered, a minimum alteration rate, noted R_{core}, can be calculated using the average radius of the grains (15 µm) as the alteration layer thickness and assuming a duration equal to the whole duration of the test to produce such a thickness. This method was also used for the AgI-$AgPO_3$-$2Bi_2O_3$ glass, which also displayed fully altered grains, as a means of comparison between the different methods. Finally, as no alteration layer was visible for the AgI-$Ag_5P_{1.5}Mo_{1.5}$-xNb_2O_5 glasses, R_{layer} could not be calculated and is therefore not reported in this table.

Glass	R ($g.m^{-2}.d^{-1}$)	R_{layer} ($g.m^{-2}.d^{-1}$)	R_{core}($g.m^{-2}.d^{-1}$)
AgI-$AgPO_3$	$4.2x10^{-2}$	0.4	n.d.
AgI-$AgPO_3$-$2Nb_2O_5$	$3.3x10^{-2}$	n.d.	1.3
AgI-$AgPO_3$-$2Bi_2O3$	$3.7x10^{-2}$	1	1.3
AgI-$Ag_5P_3O_{10}$	$2.2x10^{-2}$	0.4	n.d.
AgI-$Ag_5P_3O_{10}$-$2Nb_2O_5$	$1.5x10^{-2}$	0.2	n.d.
AgI-$Ag_5P_{1.5}Mo_{1.5}$	$1x10^{-3}$	0.4	n.d.

$AgI-Ag_5P_{1.5}Mo_{1.5}-2Nb_2O_5$	$6x10^{-4}$	n.d	n.d.
$AgI-Ag_5P_{1.5}Mo_{1.5}-5Nb_2O_5$	$9x10^{-5}$	n.d.	n.d.

Table 2. Alteration rate calculated according to various methods (uncertainty for R: 15%; uncertainty for R_{layer}: 20% (estimate))

Comparing the results from the three methods, it can be noted that those obtained from the NML clearly underestimate other values when they are available. For glasses which displayed no tracer elements, this was to be expected. However, for the $AgI-Ag_5P_3O_{10}-2Nb_2O_5$ glass, XRD results showed that phosphorus could possibly be a tracer element, as it was not part of any crystallized phase. Considering the difference of values between the two methods for this glass (about a factor of 10), it can be assumed that there is some phosphorus retention in an amorphous phase, or in a crystallized phase of which the fraction was too low to be detected by XRD, and thus that phosphorus cannot be considered as a tracer element either. The comparison between these calculation methods shows that it could be easy to underestimate the alteration of such glasses when looking only at elemental releases in solution. However, it can be seen that for the $AgI-Ag_5P_{1.5}Mo_{1.5}-xNb_2O_5$ glasses, only the elemental releases in solution were used to determine the alteration rate, thus possibly leading to a misinterpretation of the results. Elemental releases show a strong dependence on the niobium content of the glass, with a sharp decrease in the presence of niobium. This result is interpreted as the consequence of the crosslinking effect of niobium on the glass network. In fact, the glass transition temperature, as measured by differential scanning calorimetry (heating rate of 10°C.min^{-1} under air; precision +/- 2°C; results not shown here), evolves from 187°C for $AgI-Ag_5P_{1.5}Mo_{1.5}$ to 191°C for $AgI-Ag_5P_{1.5}Mo_{1.5}-2Nb_2O_5$, and to 203°C for $AgI-Ag_5P_{1.5}Mo_{1.5}-5Nb_2O_5$. However, in order to avoid an underestimation of the alteration, the $AgI-Ag_5P_{1.5}Mo_{1.5}-5Nb_2O_5$ glass alteration layer was further characterized using ToF-SIMS.

4.2. Study of the AgI-$Ag_5P_{1.5}Mo_{1.5}$-$5Nb_2O_5$ glass alteration layer

The positive and negative ion profiles obtained by ToF-SIMS analysis of the AgI-$Ag_5P_{1.5}Mo_{1.5}$-$5Nb_2O_5$ glass alteration layer are shown in Figure 9. Surprisingly, the two profiles display elements like potassium, chloride, and sodium, that were not considered as part of the original glass composition. The potassium and chloride are pollutants contributed by the pH electrode during pH measurements (KCl is used as an electrolyte with such an electrode), while sodium as well as potassium are impurities in the initial glass (added by the $AgNO_3$ reagent (main impurities of this reagent)). These three elements were only detected because of the high sensitivity of the analysis method. However, they provide precious information about glass alteration. It can be seen that K^+ and Cl^- concentrations in the alteration layer decrease down to a depth of about 1700 nm. Concerning Na^+, its concentration is very low at the surface of the sample and increases until approximately the same depth, when a plateau is reached for a concentration equal to that of the pristine glass. These results can be explained by Na diffusion in the alteration layer, leading to a release of sodium from the pristine glass due to the well-known H^+ <-> Na^+ ion-exchange interdiffusion process, and a low retention in the alteration layer. As a consequence of water diffusion, potassium and chloride are brought from the solution towards the pristine glass surface. A depth of 1700 nm is also in good agreement with the demarcation line observed on this glass in Figure 7 (within the uncertainty range for SEM measurement), this line possibly being the sign of these phenomena. The fact that no difference in chemical composition was detected by EDS on either side of the line could indicate the higher sensitivity of ToF-SIMS for trace elements like K, Cl, and Na compared to EDS, which did not identify them.

It must be noted that this water diffusion does not necessarily imply a glass network alteration going so deeply, as the glass element concentrations decreased only starting at 500 nm for phosphorous, and only at 100 nm for molybdenum and niobium.

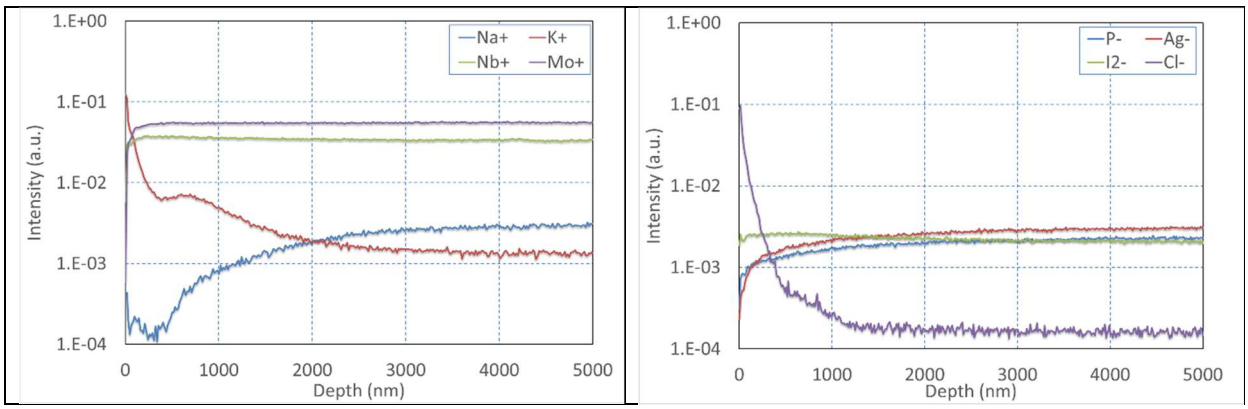

Figure 9. Positive (left) and negative (right) ion profiles obtained by ToF-SIMS analysis of the alteration layer for the AgI-$Ag_5P_{1.5}Mo_{1.5}$-$5Nb_2O_5$ glass.

Considering these results, an alteration rate based on the depth of Na diffusion (deduced from Na^+ profile when intensity is half that in the pristine glass [20]) as a measurement of the alteration layer thickness, and noted R_{Na}, can be calculated. This calculation assumes that the alteration resistance is seen as the resistance to Na diffusion, regardless of the glass network behavior. Another calculation, noted hereafter as $R_{network}$, could be applied using the depth at which the glass former network elements start to show a decrease in concentration. In this case, the depth to be used would be 500 nm. This method assumes that the alteration resistance is actually the resistance of the glass network to alteration.

Looking at these results and comparing them with the values obtained from NML (Table 3), it is clear that the alteration rate can vary by a factor of 100 between these calculation methods. In fact, the alteration layer can be seen as the concatenation of two successive layers. At the outer surface, a network former–depleted layer prevails. More in depth, it is followed by a hydrated layer within which network former concentrations are not affected,

and which corresponds to an interdiffusion area. It is worth noting that this kind of structure also exists for borosilicate glasses used for high-level nuclear waste (HLW) vitrification but in that case, the interdiffusion area can also correspond to a depletion in boron and some other elements that are poorly linked to the glass network. However, when a "pure" interdiffusion area exists (i.e. within which network formers are not affected), no congruency should be observed between alkaline elements (the ones that are exchanged during the interdiffusion process) and network formers in the earlier alteration stages. Here, a value of 3.9×10^{-3} $g.m^{-2}.d^{-1}$ ($R_{network}$) was determined for the resistance of the glass network, or of $1.6.10^{-1}$ $g.m^{-2}.d^{-1}$ for the resistance to Na diffusion. As these values are higher than that calculated based on the NML, it can be concluded that phosphorus is not a tracer element.

Glass	R ($g.m^{-2}.d^{-1}$)	R_{Na} ($g.m^{-2}.d^{-1}$)	$R_{network}$ ($g.m^{-2}.d^{-1}$)
$AgI-Ag_5P_{1.5}Mo_{1.5}-5Nb_2O_5$	9×10^{-5}	1.6×10^{-1}	3.9×10^{-3}

Table 3. Alteration rate calculated according to various methods for the $AgI-Ag_5P_{1.5}Mo_{1.5}-5Nb_2O_5$ glass (uncertainty for R: 15%; uncertainties for R_{water} and $R_{network}$: 20% (estimate))

4.3. Comparison of the alteration rates of various glasses

When trying to compare the alteration rates of these glasses, some significant differences appear between phosphate glasses and phospho-molybdate glasses. For phosphate-only glasses, the addition of a crosslinking reagent (bismuth or niobium) has little effect on the chemical durability of these glasses (taken as their resistance to phosphorus release) in the experimental conditions explored here, and even none at all for glasses of the $AgI-AgPO_3$ system. Bear in mind that these conditions were chosen to favor the formation of an alteration layer. Therefore for the phosphate-only glass, crosslinking reagents do not seem to play a significant role on the ability to form a passivating alteration layer. However for phospho-molybdate glasses, the addition of niobium has a significant effect on the retention

rates linked to the evolution of NMLs, with a substantial increase in the chemical durability (taken as their resistance to phosphorus release). As seen, in spite of the close hydration rate values between the AgI-$Ag_5P_{1.5}Mo_{1.5}$ (taken as R_{Na}) and the AgI-$Ag_5P_3O_{10}$ system (taken as R_{layer}) (0.4 – 0.16 $g.m^{-2}.d^{-1}$), NMLs for the AgI-$Ag_5P_{1.5}Mo_{1.5}$ system are noticeably lower, indicating a better retention efficiency and a better chemical durability.

The main difference that could be found during the tests of these two types of glasses is a strong pH difference between the sampled solutions. While phosphate-only glasses induced pH values below 3, that is to say very acidic pH values, phospho-molybdate glasses induced pH values between 5 and 5.5. Considering the major role played by H^+ ions during phosphate glass alteration [21][22], as the dealkalization process (i.e. interdiffusion) that exposes the glass network to hydrolysis reactions, it could be hypothesized that the very acidic pH conditions intensified the alteration of purely phosphate glasses. Thus the action of the crosslinking reagents was limited to hampering the alteration phenomenon of these glasses. For phospho-molybdate glasses, it could have been supposed that the higher pH values would have limited the dealkalization process. However, due to the close hydration rate values with those of phosphate-only glasses, this effect is not of primary importance in explaining their better chemical durability (taken as their resistance to phosphorus release). To explain such results, it should be inferred that pH also plays a role in hydrolysis reactions that follow the dealkalization process. In the case of phospho-molybdate glasses, the rate of these reactions decreased (as shown by the decrease in phosphorus release when compared with phosphate-only glasses). Moreover, in this case, a clear effect of the crosslinking action of niobium on chemical durability was observed.

5. Conclusion

The chemical durability of iodine-containing silver phosphate glasses was investigated, focusing on the effect of two crosslinking reagents (Bi_2O_3 and Nb_2O_5) on their long-term chemical durability in pure water. Alteration rates were calculated following various methods, in order to compare said methods. Results showed that alteration rates calculated using the NML are underestimated compared to those obtained using the thickness of the alteration layer. This was mainly explained by the lack of tracer elements for these systems. The investigations also showed that the two crosslinking reagents studied here have little effect on the chemical durability of phosphate-only glasses (similar values of NMLs were obtained, whatever the crosslinking reagent content). However, for phospho-molybdate glasses, the addition of Nb_2O_5 had a significant effect on their chemical durability, taken as their ability to form a passivating layer that retains most of the elements that are part of the pristine glass. For phosphorus, the more mobile element, release rates decreased by two orders of magnitude compared to phosphate-only glasses, and this trend depends on the Nb_2O_5 concentration. A preliminary explanation for the better behavior of phospho-molybdate glasses over phosphate-only glasses could well be based on the values of pH imposed by each system. Acidic conditions, corresponding to phosphate-only glasses, strengthen hydrolysis of the glass network, whereas more neutral conditions, corresponding to phospho-molybdate glasses, favor a better resistance. For the latter conditions, the effect of a crosslinking reagent such as Nb_2O_5 is emphasized. A hydrolysis rate of 3.9×10^{-3} $g.m^{-2}.d^{-1}$ was determined for 5 mol% Nb_2O_5. Given this result, and as alkaline conditions tend to prevail in low-level and intermediate-level waste repositories, the influence of higher pH values on the matrix durability will have to be clarified in future works. To be able to

conclude as to the interest of these glasses for radioactive iodine conditioning, it will also be necessary to go further, and study the chemical durability under more realistic conditions. For instance, taking the chemical composition of the water found in underground repository conditions into account could provide new insights.

6. Acknowledgments

A.-L. Chabauty thanks the CEA for her PhD grant. Chevreul Institute (FR 2638), Ministère de l'Enseignement Supérieur et de la Recherche, Région Nord – Pas de Calais and FEDER are acknowledged for kindly supporting this work**.** The authors are also grateful to V. Alaimo from ULille for her assistance with the ICP analyses.

7. References

[1]: S. Gin, P. Jollivet, M. Tribet, S. Peuget, S. Schuller, Radionuclide containment in nuclear glasses: an overview, Radiochimica Acta 105 (2017), 927-959.

[2]: B.J. Riley, M. J. Schweiger, D.-S. Kim, W.W. Lukens Jr., B.D. Williams, C. Iovin, C.P. Rodriguez, N. R. Overman, M. E. Bowden, D. R. Dixon, J. V. Crum, J. S. McCloy, A. A. Kruger, Iodine solubility in a low-activity waste borosilicate glass at 1000 °C, Journal of Nuclear Materials 452 (2014), 178–188.

[3]: B.J. Riley, J.D. Vienna, D.M. Strachan, J.S. McCloy, J.L. Jerden Jr., Materials and processes for the effective capture and immobilization of radioiodine: A review, Journal of Nuclear Materials 470 (2016), 307-326.

[4]: K. Noshita, T. Nishi, T. Yoshida, H. Fujihara, T. Murase, Vitrification technique of radioiodine waste using AgI-Ag2O-P2O5 glass system, Radioactive Waste Management and Environmental Remediation, ASME 1999 (Nagoya, Japon).

[5]: T.J. Garino, T.M. Nenoff, J.L. Krumhansl, D.X. Rademacher, Low-Temperature Sintering Bi-Si-Zn-Oxide Glasses for Use in Either Glass Composite Materials or Core/Shell ^{129}I Waste Forms, Journal of the American Ceramic Society 94[8] (2011), 2412-2419.

[6]: M.J. Plodinec, Borosilicate Glasses for Nuclear Waste Immobilization, Glass Technology 41 (2000), 186-192.

[7]: K.K. Olsen, J.W. Zwanziger, Multi-Nuclear and Multi-Dimensional Nuclear Magnetic Resonance Investigation of Silver Iodide-Silver Phosphate Fast Ion Conducting Glasses, Solid State Nuclear Magnetic Resonance 5 (1995), 123-132.

[8]: T. Minami, Y. Takuma, M. Tanaka, Superionic Conducting Glasses: Glass Formation and Conductivity in the AgI-Ag_2O-P_2O_5 System, Journal of the Electrochemical Society, 124-11(1977), 1659-1662.

[9]: H. Fujihara, T. Murase, T. Nishi, K. Noshita, T. Yoshida, M. Matsuda, Low Temperature Vitrification of Radioiodine Glasses using AgI-Ag_2O-P_2O_5 Glasses, Materials Research Society Symposium – Proceedings 556 (1999), 375-382.

[10]: T. Sakuragi, T. Nishimura, Y. Nasu, H. Asano, K. Hoshino, K. Iino, Materials Research Society Symposium Proceedings 1107 (2008), 279-286.

[11]: T. Lemesle, F. O. Méar, L. Campayo, O. Pinet, B. Revel, L. Montagne, Immobilization of Radioactive Iodine in Silver Aluminophosphate Glasses, Journal of Hazardous Materials 264 (2014), 117-126.

[12]: J. H. Yang, H.S. Park, Y.Z. Cho, Silver phosphate glasses for immobilization of radioactive iodine, Annals of Nuclear Energy 110 (2017), 208-214.

[13]: T. Lemesle, L. Montagne, F. O. Méar, B. Revel, L. Campayo, O. Pinet, Bismuth-Silver Phosphate Glasses as Alternative Matrices for the Conditioning of Radioactive Iodine, Physics and Chemistry of Glasses - European Journal of Glass Science and Technology 52 (2015), 71-75.

[14]: A.-L. Chabauty, L. Campayo, F. O. Méar, L. Montagne, Niobium- and bismuth-silver phosphate glasses for the conditioning of radioactive iodine, Journal of Non-Crystalline Solids
510 (2019), 51-61.

[15]: Agence Nationale pour la gestion des Déchets RAdioactifs (ANDRA), Dossier Argile 2005 : Tome – Safety Evaluation of a Geological Repository, Reports Series No. 270VA, ANDRA, Paris, 2005.

[16]: P. Frugier, Y. Minet, N. Rajmohan, N. Godon, S. Gin, Modeling glass corrosion with GRAAL, npj Materials Degradation 2[1] (2018), 1-13.

[17]: P.P. Poluektov, O.V. Schmidt, V.A. Kascheev, M.I. Ojovan, Modelling aqueous corrosion of nuclear waste phosphate glass, Journal of Nuclear Materials 484 (2017), 357-366.

[18]: M. Fournier, S. Gin, P. Frugier, Resumption of nuclear glass alteration: State of the art, Journal of Nuclear Materials 448[1-3] (2014), 348-363.

[19]: E. Vernaz, S. Gin, C. Jégou, I. Ribet, Present understanding of R7T7 glass alteration kinetics and their impact on long-term behavior modeling, Journal of Nuclear Materials 298 (2001), 27-36.

[20]: C. Jégou, S. Gin, F. Larché, Alteration kinetics of a simplified nuclear glass in an aqueous medium: effects of solution chemistry and of protective gel properties on diminishing the alteration rate, Journal of Nuclear Materials 280 (2000), 216-229.

[21]: N. Donzel, S. Gin, F. Augereau, M. Ramonda, Study of gel development during SON68 glass alteration using atomic force microscopy. Comparison with two simplified glasses, Journal of Nuclear Materials 317 [1] (2003), 83-92.

[22]: J. Schindelin, I. Arganda-Carreras, E. Frise, V. Kaynig, M. Longair, T. Pietzsch, S. Preibisch, C. Rueden, S. Saalfeld, B. Schmid, J.-Y. Tinevez, D. J. White, V. Hartenstein, K. Eliceiri, P. Tomancak and A. Cardona, Fiji: an open-source platform for biological-image analysis, Nature Methods 9-7 (2012), 676-682.

[23]: D. R. Lide, Handbook of Chemistry and Physics, 85th edition, Ed. CRC Press, Boca Raton (Florida (US)), 2004.

[24]: S. Gin, P. Jollivet, G. Barba Rossa, M. Tribet, S. Mougnaud, M. Collin, M. Fournier, E. Cadel, M. Cabie, L. Dupuy, Atom-Probe Tomography, TEM and ToF-SIMS study of borosilicate glass alteration rim: A multiscale approach to investigating rate-limiting mechanisms, Geochimica et Cosmochimica Acta 202 (2017) 57–76

[25]: B. C. Bunker, G. W. Arnold et J. A. Wilder, Phosphate glass dissolution in aqueous solutions, Journal of Non-Crystalline Solids 64 (1984), 291-316.

[26]: H. Gao, T. Tan and D. Wang, Dissolution mechanism and release kinetics of phosphate controlled release glasses in aqueous medium, Journal of controlled release 96 (2004), 29-36.